

Femtosecond dynamics of ballistic charge current gratings in GaAs

Y. Kerachian, P. A. Marsden, A. Najmaie, J. E. Sipe and H. M. van Driel

Department of Physics, University of Toronto, Toronto, Ontario M5S1A7, Canada
vandriel@physics.utoronto.ca

Arthur L. Smirl

Laboratory for Photonics and Quantum Electronics, 138 IATL, University of Iowa, Iowa City, Iowa 52242, USA

Abstract: We investigate the dynamics of ballistic charge currents, optically-injected into GaAs by quantum interference of 1550 and 775nm, 150fs pulses. Space-charge induced transport and ambipolar diffusion successively define the relaxation dynamics on a 500fs-20ps timescale.

©2005 Optical Society of America

OCIS codes: 320.7130 Ultrafast processes in condensed matter, including semiconductors; 270.1670 Coherent optical effects; 190.4720 Optical nonlinearities in condensed matter.

Coherent control techniques provide an all-optical basis for the generation and control of charge and spin degrees of freedom in semiconductors. Quantum interference between optical absorption pathways can be used to control, *e.g.*, carrier density and spin population or charge currents and spin currents[1-5]. When the interference schemes involve pulses that are not co-propagating in the semiconductor it is possible to induce transient spatial gratings of populations or currents and obtain information about their spatio-temporal dynamics. Earlier we showed how pure spin current gratings could be produced in GaAs at room temperature using interference between single and two photon absorption processes induced by non-copropagating 775 and 1550 nm, *orthogonally* polarized, 150 fs pulses[3]. In that case grating amplitude decay on a 3 ps timescale was attributed to spin diffusion governed by the electron diffusion ($195 \text{ cm}^2\text{s}^{-1}$). Here, using *parallel* polarized pulses under otherwise the same conditions we are able to generate ballistic pure electrical currents. The subsequent dynamics reveal the strong roles played by carrier cooling, dielectric relaxation and ambipolar diffusion following ballistic charge separation.

The experimental setup for inducing and monitoring the charge current gratings is shown in Fig. 1.

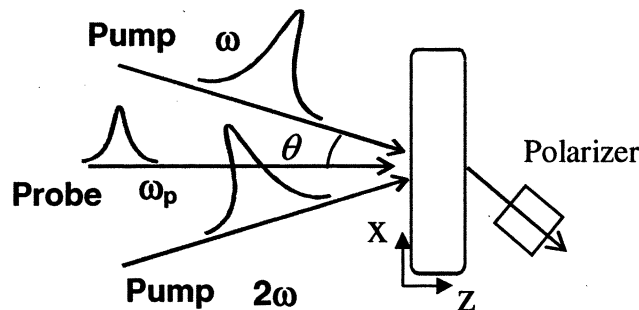


Fig. 1: Experimental setup. The two p-polarized pump beams at frequencies ω and 2ω are incident on the sample at a half angle of $\theta=10^\circ$ and form a current grating. An s-polarized probe pulse at frequency ω_p is diffracted from this grating and the s-polarized component of the diffracted beam is detected.

Pump pulses at frequencies ω (1550 nm) and 2ω (775 nm) propagating at angles of 10° on either side of the normal to the surface, are incident on a (001) cut, 800 nm thick piece of GaAs at 295 K. The pulses are p-polarized along the crystal (100) axis and temporally and spatially overlapped with a spot size (FWHM) of $50 \mu\text{m}$ on the surface. For this geometry electrical currents are injected along the crystal (100) direction through the quantum interference between the two beams' absorption amplitudes [2] with the local current amplitude and direction dependent on the relative phase $2\phi_\omega - \phi_{2\omega}$. Because of the pump beam geometry, the current varies sinusoidally along the (100) axis with a period of $\Lambda=2.2 \mu\text{m}$; in other words, a current grating is formed. It should be stressed that there is no initial carrier density modulation – only the velocities of the carriers are modulated. However, since electrons and holes move in opposite directions,

electron and hole density gratings are formed which differ by π in phase. Time delayed s-polarized 830 nm 150 fs pulses are focused at near-normal incidence to $35 \mu\text{m}$ onto the centre of the pump beams' spot. This probe beam is diffracted by any density grating formed in the sample and the s-polarized component is detected by a photomultiplier tube (PMT). The diffracted intensity measures the efficiency of the grating produced by the two pump beams, and hence the modulation depth of the grating. For incident pump intensities of 5 and 0.3 GWcm^{-2} at 1550 and 775 nm respectively the two absorption pathways are balanced and produce a peak carrier and current density of 10^{18} cm^{-3} and 60 kAcm^{-2} respectively. We have specifically chosen the pump beams' polarization and crystal geometry so as to only generate a ballistic charge current grating. This configuration suppresses any carrier population grating that might be generated via a coherent control $\chi^{(2)}$ based interaction [3,4].

The results of the experiment are shown in Figs. 2a and b on different time scales. Near zero time delay between pump and probe pulses the grating efficiency rises rapidly, essentially following the shape of the pump-probe cross-correlation trace (also shown on the figure). This initial feature is seen to decay on a timescale of ~ 500 fs. The grating diffraction efficiency then rises on a picosecond timescale, peaks near 5 ps delay and then decays on a 10 ps time scale.

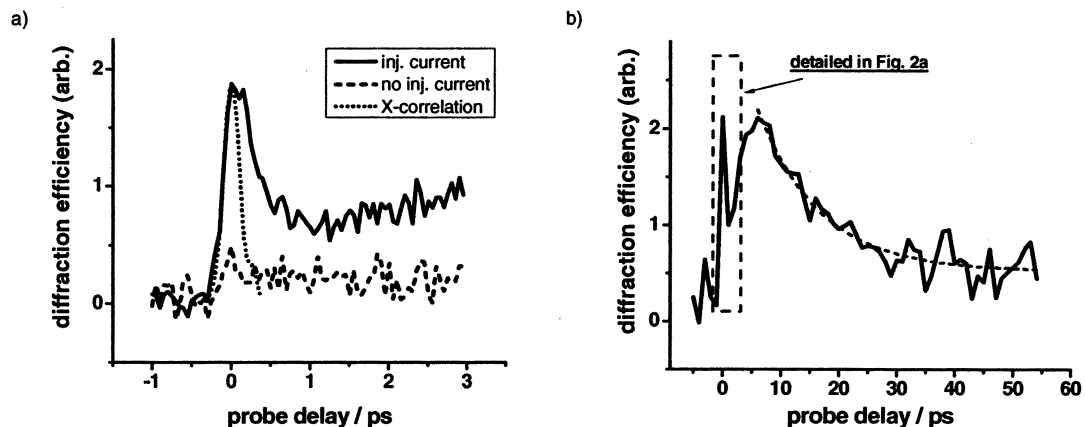


Fig. 2: Diffraction efficiency as a function of pump-probe time delay. a) The evolution of the diffraction efficiency following injection of a ballistic current by co-polarized pump beams (solid trace). The dashed curve are data from the same experiment with orthogonally polarized pump beams. The dotted curve is the cross-correlation between the probe pulses and those at frequency ω . b) Time evolution of the current grating on longer timescales showing the fast response of the current grating (spike near zero delay) and the slow decay of the resultant population grating by ambipolar diffusion. The dashed curve represents a trace with the same decay time as the population grating data in Fig. 4.

Also shown in Fig. 2a are the results of an experiment using crossed linear polarization pump pulses; the injected charge current grating is very small as expected [2].

The evolution of the grating efficiency can be understood in terms of the following steps (See Fig. 3).

- I) At early times we attribute the ultrafast response to electrons and holes quickly separating to form a carrier density grating and establishing a space-charge field.
- II) The generated quasi-electrostatic field causes carriers to decelerate rapidly through dielectric relaxation processes and reverse direction; this causes partial collapse of the grating on a 500 fs time scale. This field driven transport process is influenced by the carrier mobility which depends on the momentum scattering time, a carrier density and temperature dependent parameter.
- III) Since the hole effective mass is much larger than the electron mass, holes as well as surrounding electrons do not return to the region where they were generated. This results in a neutral carrier density modulation with the carrier temperature not at the lattice temperature.
- IV) The hot carrier density modulation continues to cool to the 295 K lattice temperature in a time of a few picoseconds. With cooling, the electrons increasingly occupy states near the conduction band minimum to which the 830 nm probe pulse is sensitive. The cooling process induces the second, slower rise in diffraction efficiency which subsequently decays because of carrier ambipolar diffusion. The scenario outlined in this phase agrees with measurements of the decay of directly-

written density modulation gratings formed via a $\chi^{(2)}$ interaction (shown in Fig. 4) where there again is a slow rise of the diffraction efficiency and the decay time is ~ 10 ps. Such a decay time is consistent with the known ambipolar diffusion coefficient of $63 \text{ cm}^2\text{s}^{-1}$.

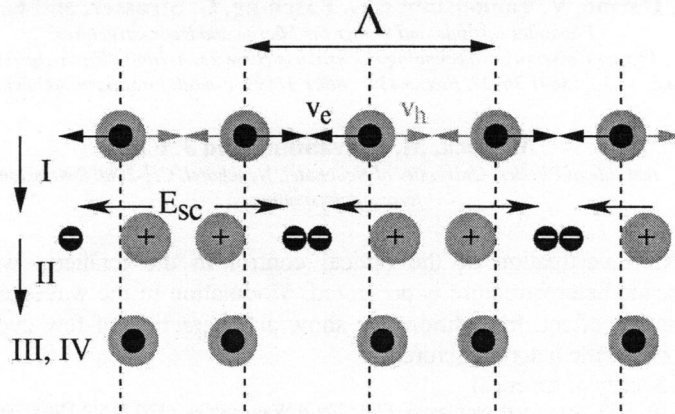


Fig. 3: Schematic diagram of grating formation. I) Electrons (black circles) and holes (grey circles) are injected in opposite directions (velocities v_e and v_h) and set up a space-charge field (E_{sc}). II) Carriers decelerate in the field and reverse direction causing the grating to partially collapse. III) The large hole mass causes a electron-hole pair population grating to form. IV) Hot carriers cool increasing grating strength and ultimately the grating decays by ambipolar diffusion.

In considering phase II, from the measured electron and hole mobilities at room temperature ($7900 \text{ cm}^2\text{V}^{-1}\text{s}^{-1}$ and $2500 \text{ cm}^2\text{V}^{-1}\text{s}^{-1}$, respectively), we estimate a 1 fs dielectric relaxation time for our carrier density and for a static relative dielectric constant of 13. A much lower mobility is therefore required to explain the 500 fs grating decay time measured in this experiment for which a carrier collision time of the order of 10 fs is needed. However, more rapid momentum scattering is not unreasonable in our case since immediately after the excitation process the effective temperature of the carriers is approximately 10^3 K, they have access to a much larger density of states than near the edge of their bands, and the carrier density is in a regime where carrier-carrier scattering processes are expected to contribute.

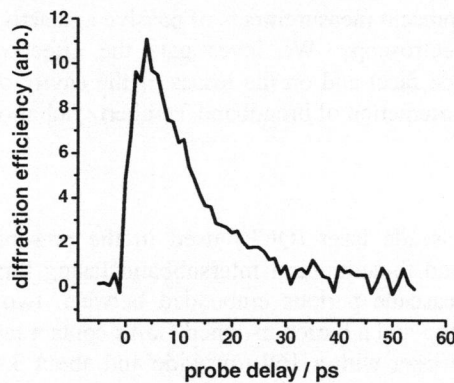


Fig. 4: Diffraction efficiency as a function of pump-probe time delay for a directly-written population grating

In summary we have provided insight into how electrical currents, generated in small volumes and on ultrafast time scales relax, and have observed the role of dielectric relaxation, carrier cooling and ambipolar diffusion.

References

- [1] M.J. Stevens *et al.*, in *Optics of Semiconductors and Their Nanostructures*, H. Kalt and M. Hetterich, eds. (Springer, Berlin, 2004), pp. 209-245.
- [2] A. Haché *et al.*, *Phys. Rev. Lett.* **78**, 306 (1997).
- [3] Y. Kerachian, P. Nemeč, H.M. van Driel and A.L. Smirl, *J. Appl Phys.* **96**, 430 (2004).
- [4] J.M. Fraser, A.I. Shkrebtii, J.E. Sipe and H.M. van Driel, *Phys. Rev. Lett.* **83**, 4192 (1999).
- [5] R.D.R. Bhat and J.E. Sipe, *Phys. Rev. Lett.* **85**, 5432 (2000).